ELSEVIER

Journal of Chromatography A, 923 (2001) 215–227

JOURNAL OF CHROMATOGRAPHY A

www.elsevier.com/locate/chroma

Preparation and characterization of monolithic polymer columns for capillary electrochromatography

T. Jiang, J. Jiskra, H.A. Claessens*, C.A. Cramers

Laboratory of Instrumental Analysis, Department of Chemical Engineering and Chemistry, Eindhoven University of Technology, P.O. Box 513, 5600 MB Eindhoven, The Netherlands

Received 2 March 2001; received in revised form 18 May 2001; accepted 18 May 2001

Abstract

A series of micro-monolithic columns with different porosities were prepared for capillary electrochromatography (CEC) by in-situ copolymerization of butyl methacrylate, ethylene glycol dimethacrylate, and 2-acrylamido-2-methyl-1-propanesulfonic acid in the presence of a porogen in fused-silica capillaries of 100 μm I.D. Different column porosities were obtained by changing the ratios of monomers to porogenic solvents. Columns were investigated and evaluated under both pressure-driven (high-performance liquid chromatography, HPLC) and electro-driven (capillary electrochromatography, CEC) conditions. Each column exhibited different efficiency and dependency on flow velocity under electro-driven conditions. Abnormally broad peaks for some relatively bulky molecules were observed. Possible explanations are discussed. The differences in column efficiency and retention behavior between the two eluent-driven modes were studied in detail. In addition, other column properties, such as morphology, porosity, stability and reproducibility, were extensively tested.

Keywords: Electrochromatography; Monolithic polymer column; Porosity; Micropore

1. Introduction

Capillary electrochromatography (CEC) has emerged as a promising micro-separation technique that combines chromatographic selectivity with high efficiency and miniaturization potential of capillary electrophoresis (CE) [1–6]. To date, a number of papers have been published on the theoretical and practical aspects of CEC [3,7–30]. However, some technical problems including column preparation have slowed down its development and widespread implementation [31,32]. Most columns used nowadays in CEC are packed in a similar way as in micro-HPLC. High experimental skill and experience is required to reproducibly pack micron-sized particles into a narrow-bore tube and to prepare a solid and stable frit at both ends of the column. Additionally, it is extremely difficult to avoid side effects arising from frits [17], i.e. bubble formation and heterogeneity of the electrical field across the column. Furthermore, there are only a few commercially available stationary phases dedicated for CEC which are expected to provide sites for the required interactions as well as the charged group for generation of the electroosmotic flow, EOF [30]. All these technical problems have stimulated the de-

*Corresponding author. Tel.: +31-40-247-3012; fax: +31-40-245-3762.

E-mail address: h.a.claessens@tue.nl (H.A. Claessens).

0021-9673/01/$ – see front matter
PII: S0021-9673(01)00982-7

velopment of various alternative approaches [33–48]. Among these, one competing strategy is to prepare monolithic media by in-situ polymerization within the confine of a mold. This approach has recently attracted substantial attention in view of its capability to eliminate the difficulties described above for making packed columns [37–49]. Presently, there exist two main types of monolithic materials, silica sol–gels [37–40] and porous organic polymers. In principle, the polymeric approach exhibits more potential advantages and a more promising future compared to its silica-based counterparts. This is due to the simpler preparation process, higher efficiency, easier pore size control, and more facile adaptability to adjust column selectivity, as well as the direction and the speed of the electro-osmotic flow (EOF) offered by polymer rods. Several groups have spent considerable effort in this field [41–49]. However, this technique is still virtually in its infancy. Until now, most applications have concentrated on simple small neutral compounds. Moreover, the physico-chemical properties of these porous polymers under electric field conditions are still not straightforward to be explained.

In this study, we prepared a series of polyalkylmethacrylate-based monolithic capillary columns with different permeabilities. The column performances under both CEC (electro-driven, ED) and HPLC (pressure-driven, PD) were evaluated and compared in detail. In addition, the micropore size distributions in these polymeric monoliths were investigated, and some practical and theoretical problems associated with these types of rods are also discussed.

2. Experimental

2.1. Chemicals

Butyl methacrylate (BMA), ethylene glycol dimethacrylate (EGDMA), 2-acrylamido-2-methyl-1-propanesulfonic acid (AMPS) and 3-(trimethoxysilyl)propyl methacrylate were obtained from Aldrich. Acetonitrile (ACN) and tetrahydrofuran (THF) with HPLC grade purity were from Biosolve (Valkenswaard, The Netherlands). Polystyrene standards were obtained from DuPont (Wilmington, DE) and all the analytes and other chemicals were from Merck (Darmstadt, Germany). Fused-silica tubing (100 μm I.D.) was purchased from Polymicro Technologies (Phoenix, AZ, USA). The mobile phase was composed of 20% (v/v) sodium phosphate buffer (5 m*M*, pH 7) and 80% (v/v) ACN. It was degassed by ultrasonication and filtered through a filter (pore size, 0.45 μm) before use.

2.2. Column preparation

The monomers (60.0 wt% BMA, 39.7 wt% EGDMA and 0.3 wt% AMPS), azobisisobutyronitrile (AIBN) used as a polymerization initiator (1 wt% with respect to the total monomer amount) and porogen (1-propanol, 1,4-butanediol and 10 wt% water) were mixed ultrasonically into a homogenous solution [50–52]. For different columns, different porogen concentrations and volume fractions were used, as detailed in Table 1. Subsequently, the reactant solution was purged with nitrogen for 3 min before a small part of the reactant mixture was introduced into a capillary (unmodified or silanized) by a 10-μl syringe. The capillary was either filled completely or to a certain distance from one end. After both ends of the capillary were sealed in a micro-connector, it was kept at 60°C in an oven for 24 h. All columns were conditioned by mobile phase using a syringe pump prior to HPLC and CEC experiments.

To investigate eventual wall effects, the inner wall of some capillaries was modified before the introduction of the reactant mixture [53]. The procedure was as follows: the unmodified fused-silica capillary was first washed then filled with 1 *M* sodium hydroxide solution, both ends were put in a sealed vial filled with sodium hydroxide solution, and the capillary was then kept at 95°C for 2 h in an oven. Thereafter, the capillary was washed with ca. 60 column-volumes of deionized water and then with the same volume of acetone. The capillary was dried at 60°C under purging nitrogen for 1 h, followed by rinsing with 10 column-volumes of a silanizing solution, a solution of 50% (v/v) of 3-(trimethoxysilyl)propyl methacrylate in *N*,*N*-dimethylformamide (DMF) containing 0.02% (w/v) of hydroquinone (an inhibitor). After both ends of the capillary were sealed, it was heated in an oven at 100°C for about 8

Table 1
Characteristics of different columns

Column	Porogen[a] fraction (vol%)	Conc. of 1-propanol in porogen (wt%)	Capillary	Globule size[b] (nm)	Porosity (ϵ_T)	C%[d]	H in CEC (μm)[e]
a	47	62	Unmodified	150	0.50	0.0	6.7
b	52	62	Unmodified	250	0.56	0.0	8.3
c	57	62	Unmodified	300	0.61	0.3	10.0
d	62	62	Unmodified	800	0.67	2.0	11.0
e	67	62	Unmodified	1200	0.72	3.2	33.3
f	62	60	Unmodified	1200	NM[c]	NM	30.0
g	62	63	Unmodified	450	NM	NM	12.0
h	57	62	Modified	300	NM	0.1	10.0

[a] Porogen volume fraction in reactant solution.
[b] Microglobule size estimated from SEM pictures.
[c] NM, not measured.
[d] Compressibility, $C\% = 100 \times (L_0 - L_1)/L_0$. L_0: initial column length; L_1: column length after high pressure was applied.
[e] Plate height (H) under CEC conditions. Column efficiency was calculated by half peak-width method.

h, and then washed with DMF and acetone. Finally, the capillary was again dried with a nitrogen stream.

2.3. Instrumentation

CEC experiments were performed on a ^{3D}CE system (Agilent Technologies, Waldbronn, Germany) equipped with a DAD 1050 UV detector and an external pressure device for CEC. Control of the chromatographic system and data acquisition were carried out by a Chemstation system. Samples were injected electrokinetically. The cassette temperature was set at either 21 or 30°C. The detection wavelength was 205 nm. During each run 8 bar pressure was applied at two ends of the column.

The μ-HPLC system was composed of an ISCO model 100 DM syringe pump (Isco, Inc., Lincoln, NE, USA), a microUV–Vis SSI 500 detector (Scientific Systems, Inc., State College, PA, USA) and a Rheodyne injector (VICI AG, Valco Europe, Schenkon, Switzerland) with a 100-nl internal loop. A TEE-piece after injector with a 1 m×25 μm (I.D.) capillary was used as a splitter. The split ratio was typically 100:1. All the experiments were performed at room temperature (ca. 21°C).

The column morphology was studied by a Model JSM-840A scanning electron microscope (SEM) (JEOL, Inc., Tokyo, Japan). Samples of 5-mm long rod pieces were cut from the columns, placed on an aluminum stub via a double-sided carbon tape, and sputter-coated with a gold/palladium alloy using SPI Sputter for 4 min at 30 mA. The measurements were carried out at 10 kV at a filament current of 40 mA. According to SEM pictures the macropore sizes in the capillary rods were estimated. The micropore size distribution of the polymer was measured by BET nitrogen sorption method on an ASAP 2010 instrument (Micromeritis, Norcross, GA, USA). The equilibrium interval was 30 s, and the low-pressure dose was 0.5 g/cm^3 STP. The calculation for the micropore size is based on the slit pore model. The samples were polymers made in a 2-ml bottle by the same polymerization process as used for the corresponding columns. Before measurement, the bulk polymer was cut into small pieces, Soxhlet-extracted with methanol for 12 h, vacuum-dried for 2 days and degassed for 5 h at 65°C.

3. Results and discussion

3.1. Column efficiency in CEC

The lowest plate height (H) at the test alkyl benzenes for each column is presented in Table 1. From comparing the efficiencies of columns *d*, *f* and

g with different 1-propanol content but the same porogen volume fraction, it is clearly shown that column efficiency is very sensitive to the amount of 1-propanol. This is consistent with earlier reported results [50–52]. The column with 62 wt% 1-propanol provided the highest efficiency. Therefore, for all other columns in this study, the porogen with 62 wt% 1-propanol was chosen.

Fig. 1 shows the plots of plate height as a function of eluent velocity for alkyl benzene compounds on columns *a–e* prepared using different porogen volume fractions. As porogen volume fraction decreases from 67% (column *e*) to 47% (column *a*), the column efficiency increases from about 30 000 to 150 000 plates/m (Table 1), the steepness of all plots decreases, and the optimal flow velocity increases from less than 1 to about 6 cm/min. In addition, it is interesting to note that, for columns *a* and *b* with a lower porogen content, the column efficiency remains almost constant, regardless of the different retention factors (*k*) for all of the test compounds with retention factor (*k*) up to 6.5. This suggests that with such columns rapid separations can be obtained without loss in resolution.

In order to understand the differences in column efficiency in columns *a–e*, the polymer morphology in the capillaries was examined by scanning electron microscope (SEM). As an example, some SEM photos are shown in Fig. 2. According to the SEM pictures, the connecting microglobule size of the polymer was estimated, and presented in Table 1. The structures of the various monolithic columns differ significantly, and strongly depend on the porogen content in the reactant solutions. With the decrease in the porogen content, the microglobules become smaller (from about 1 μm for column *e* down to 150 nm for column *a*), and the globule stacking and the channel distribution become more uniform. Obviously, for the columns with lower porogen concentration, the Eddy diffusion is smaller and the mass transfer is faster, resulting in higher efficiencies and less steep Van Deemter curves.

3.2. Selectivity and retention in CEC

Apart from column efficiency, column selectivity and the retention mechanism for columns *a–e* were investigated as well. The retention mechanism of reversed-phase liquid chromatography (RPLC) of benzene derivatives for these polymer monoliths has been described in literature [50–52]. In the first instance, reversed-phase retention of neutral compounds is determined by the hydrophobicity of the stationary phase, which can be estimated by the intercept of the linear plot of carbon numbers of alkyl substitutes of alkylbenzenes as their log *k*-values under similar eluent conditions. For example from Fig. 3 column *a* clearly is more hydrophobic compared to column *b*. Furthermore, in Fig. 3, the plots for all columns have the same slope, suggesting that all the columns made from different ratios of porogen to monomers show similar CH_2-selectivity [54].

Fig. 4 presents the effect of porogen content on the distribution constant (*K*) of each test compound on the different columns. *K*-values were calculated using the experimentally obtained retention factors and the phase ratios (β) of the columns ($K=k\beta$, β-values were calculated from column porosity, ϵ_T). Obviously, the tested mono-substituted benzene derivatives have similar *K*-values on the different columns. As a result, the retention mechanism for these mono-substituted benzene compounds is the same. In contrast, for multi-substituted benzenes, especially with bulky groups, e.g. 1,3,5-triisopropylbenzene (TIPB, compound No. 7), a large difference in retention between column *e* and columns *a–d* is observed. On column *e*, TIPB is eluted extremely quickly, even earlier than benzene; 1,3-diisopropylbenzene (DIPB) is also eluted earlier in comparison with the other columns. It appears that, besides the reversed-phase retention, column *e* simultaneously exhibits size exclusion retention for relatively bulky compounds.

The micropore size distribution of the polymers was investigated by BET nitrogen sorption method as described in the Experimental section. As shown in Fig. 5, the size range of micropores is similar for columns *a–d*, around 10 Å. Column *e*, however, has a wider range of pore size distribution ranging from 8 to 30 Å. Furthermore, the total amount of micropores in columns *a–e* is significantly different. Generally, at higher porogen contents a lower amount of micropores is formed. For example, from Fig. 5, column *a* contains the highest amount of micropores while column *e* has almost no micro-

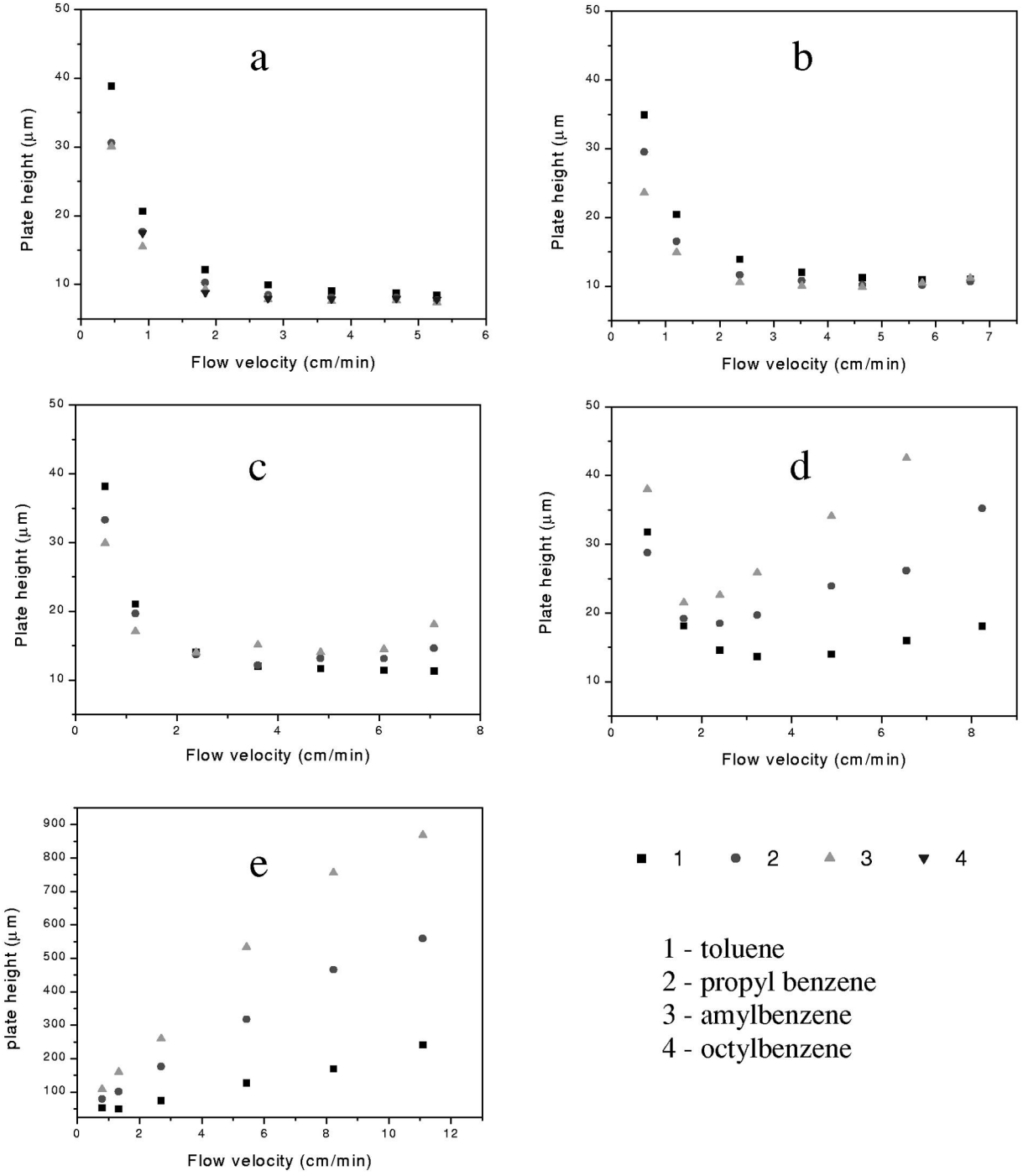

Fig. 1. Plots of plate height as a function of flow velocity in CEC mode for columns *a–e*. Conditions: the active lengths of column *a–e* are 40, 40, 40, 25, 21 cm, respectively; sample: thiourea (t_o marker), toluene, propylbenzene, amylbenzene and octylbenzene; injection: 5 kV for 3 s; applied voltages: for columns *a–d*, 30, 25, 20, 15, 10, 5 and 2.5 kV, for column *e*, 20, 15, 10, 5, 2.5 and 1.5 kV; cassette temperature, 30°C; eluent: 20% (v/v) sodium phosphate buffer (5 m*M*, pH 7) and 80% (v/v) ACN.

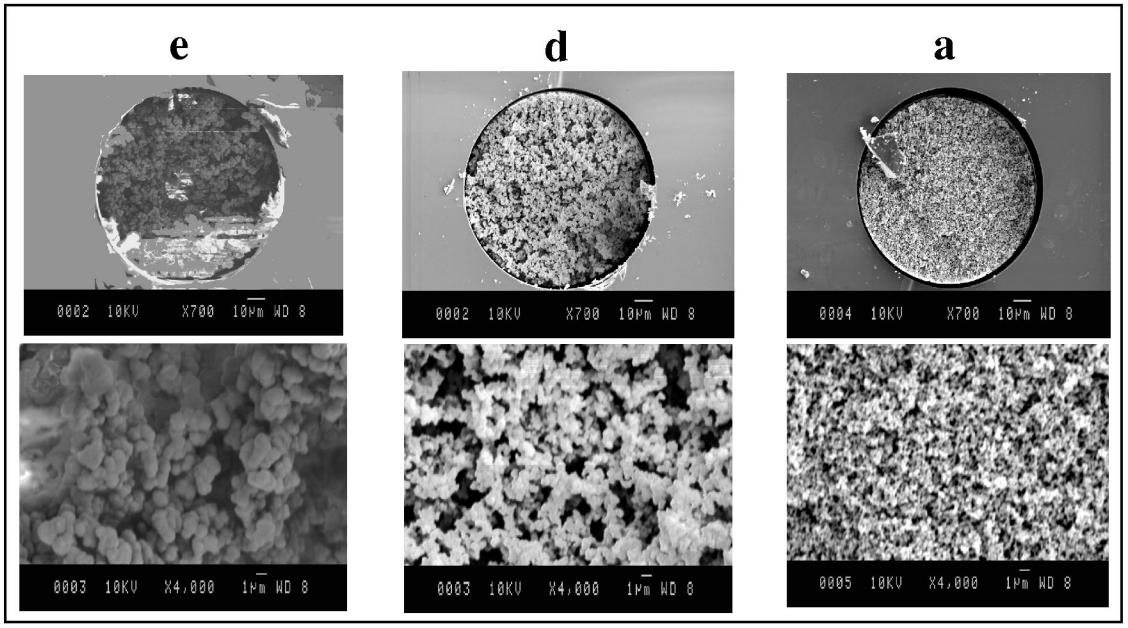

Fig. 2. Scanning electron microscope (SEM) pictures of columns *a*, *d* and *e*.

pores and its surface area is only 4.6 m^2/g (column *a* 41.3 m^2/g; column *b* 33.9 m^2/g; column *c* 13.6 m^2/g; column *d* 5.4 m^2/g). Theoretically, micropores in monolithic column have the same function as the inner pores in conventional porous packing particles, viz. they are the main areas where chro-

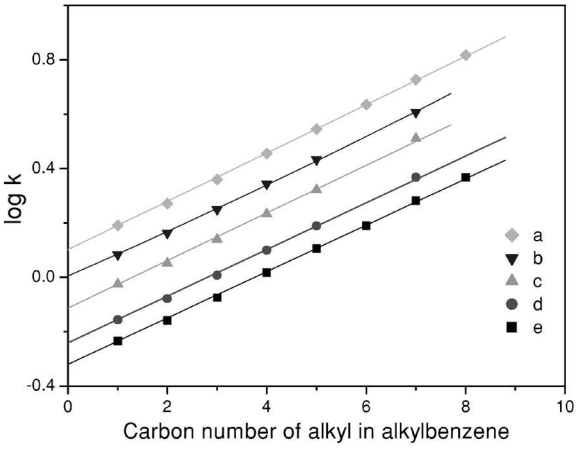

Fig. 3. Plots of the carbon numbers of the alkyl substitutes of alkylbenzene versus their log *k*-values for the columns *a–e*. Applied separation voltage is 25 kV. Other conditions as in Fig. 1.

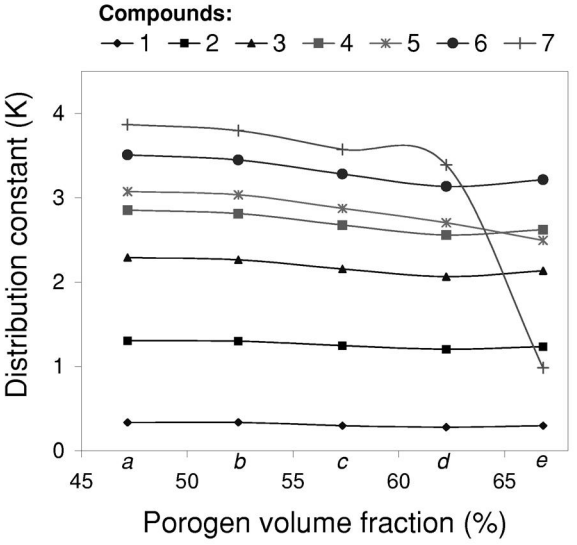

Fig. 4. Effect of porogen content on the distribution constant (*K*) of each test compound. Solutes are thiourea, benzylalcohol (1), benzene (2), propylbenzene (3), butylbenzene (4), 1,3-diisopropylbenzene (5), amylbenzene (6) and 1,3,5-triisopropylbenzene (7). Phase ratios were calculated from: $\beta = \epsilon_T/(1-\epsilon_T)$ where ϵ_T is porosity, see Table 1. Other conditions as in Fig. 1.

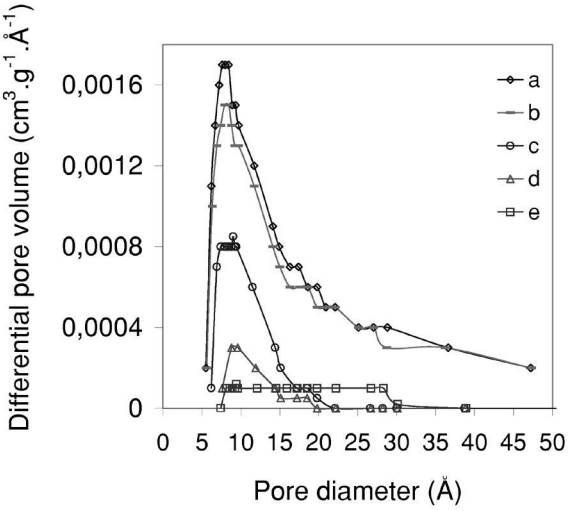

Fig. 5. Micropore size distribution for columns *a–e* measured by BET nitrogen sorption; slit pore model is used for micropore calculation.

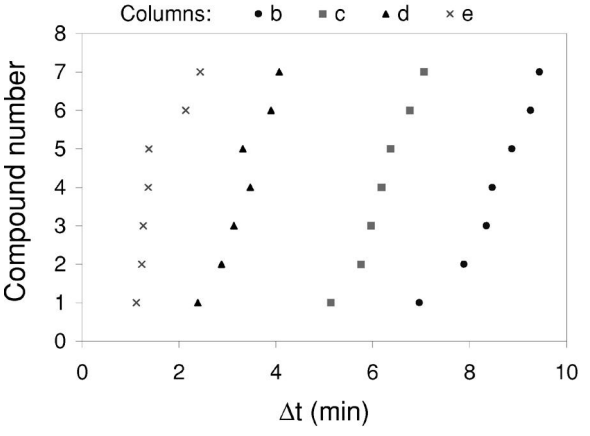

Fig. 6. Δ*t*-values (retention time of analyte minus the retention time of polystyrene MW 2 700 000, $t-t_e$) for different analytes under SEC conditions on columns *b–e*. Samples: 1, polystyrene (MW, 540); 2, TIPB; 3, *o*-terphenyl; 4, DIPB; 5, triphenylene; 6, biphenyl; 7, 1,3,5-trimethylbenzene. Mobile phase: THF.

matographic retention occurs. However, if the analytes are relatively large compared to the micropores, such as TIPB with sizes of 9×9×4.5 Å, the probability of these compounds to enter micropores becomes smaller due to steric hindrance and thus bulky analytes are prone to partial exclusion, which is more obvious on columns with lower amount of micropores. To illustrate this, on column *e*, TIPB is eluted much earlier than on the other columns containing more micropores (Fig. 4). Considering that the polymers in the measurements of BET nitrogen sorption were in the dry state, size exclusion liquid chromatography (SEC) was used to further investigate the size exclusion behaviors of compounds such as TIPB and DIPB using tetrahydrofuran (THF) as the mobile phase. In Fig. 6, Δ*t*-values of various analytes are studied where Δ*t* equals the value of $t-t_e$ where *t* is the retention time of a specific analyte and t_e is the retention time of polystyrene with a molecular mass of 2 700 000. Apparently, due to size exclusion, the Δ*t*-values of TIPB and DIPB are smaller than those of comparable small molecules. Obviously from Fig. 6, on columns with decreasing porogen content (columns *e*>*d*>*c*>*b*>*a*), Δ*t* becomes larger and the resolution for the test compounds is somewhat better. This results from the gradually larger number of micropores of these columns, which also is in good agreement with the BET results. Additionally, from the smaller Δ*t*-value of TIPB (9×9×4.5 Å) compared to triphenylene (9.2×9.2×2 Å), it can be concluded that the micropores in the polymer rods are of a slit rather than a cylinder type of shape. Therefore, the slit model was chosen to calculate the micropore size of our rod columns.

As discussed above, columns *a–d* primarily show a reversed-phase retention mechanism. As an example, a chromatogram of alkylbenzenes on column *c* is given in Fig. 7. Interestingly, abnormally broad peaks for DIPB and especially TIPB were obtained;

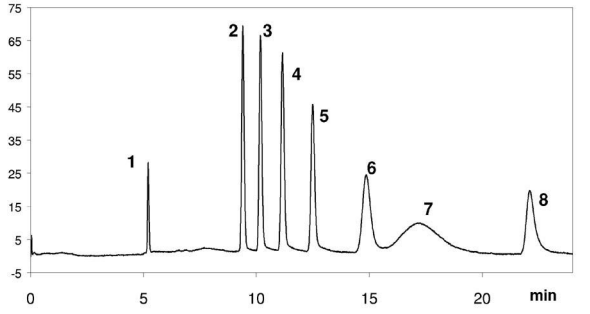

Fig. 7. CEC chromatogram on column *c*. Sample is composed of thiourea (1), benzene (2), toluene (3), ethylbenzene (4), propylbenzene (5), DIPB (6), TIPB (7) and heptylbenzene (8). Applied voltage, 30 kV. Other conditions are as in Fig. 1.

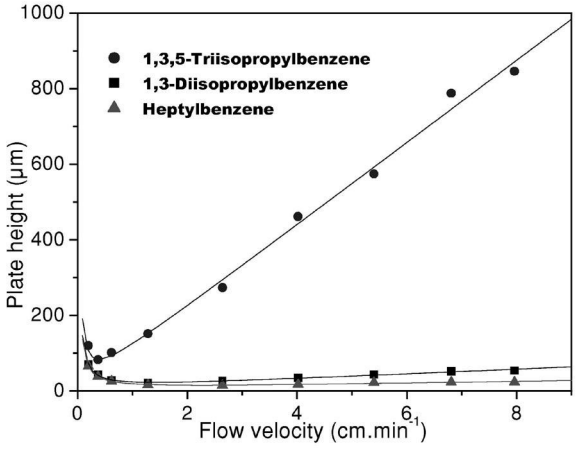

Fig. 8. Plots of plate height as a function of flow velocity for column *c*. Sample consists of TIPB (1), DIPB (2) and heptylbenzene (3). Other conditions are as in Fig. 1.

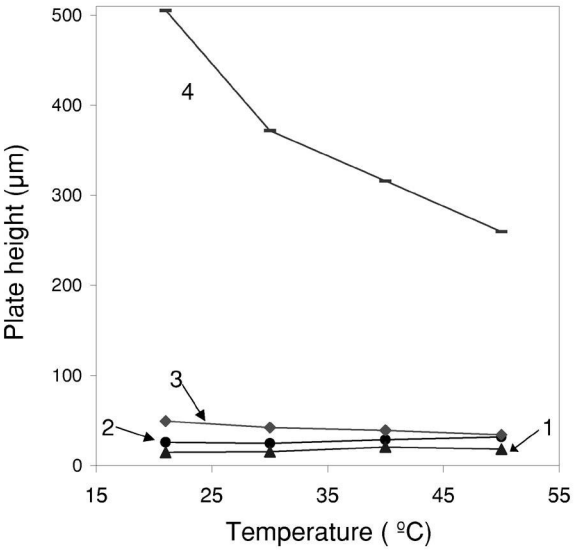

Fig. 9. Effect of temperature on plate height for column *c*. Solutes: 1, thiourea; 2, propylbenzene; 3, DIPB; 4, TIPB. Other conditions are as in Fig. 1.

similar broad peaks were also observed on columns *a*, *b* and *d* (plate height of TIPB: column *a*, 24 μm; column *b,* 39 μm and column *d,* 11 500 μm). To illustrate this in more detail, in Fig. 8 the plate height versus flow velocity for TIPB, DIPB and heptylbenzene are plotted. The Van Deemter *C*-term values for these compounds are 109.1, 6.4 and 2.4×10^{-4} min, respectively, which were calculated from the fitted curve. TIPB shows an extremely slow mass transfer, which leads to a substantial dependence of *H* on flow velocity of these compounds. In contrast, the small molecule heptylbenzene shows very low velocity dependence. As a consequence, *H*-values are satisfactory and between 21 and 35 μm in the optimal velocity span. Similar plate height function was also observed on the other columns. We assume that the slow mass transfer of TPIB results from the small micropores (ca. 1 nm) in the polymer rod that are too small for TIPB to easily enter and exit. Further evidence can be obtained from Fig. 9 of the plots of plate height versus temperature. For TIPB, there is a strong dependency of the plate height (*H*) on temperature: *H* decreases dramatically with increasing temperature, and the plate height of DIPB also shows similar tendency. However, the temperature dependency of *H*, for the small compounds, is very small. It must be emphasized here that the linear relationship between voltage and current suggests that Joule heating is negligible (Fig. 10). We believe that Joule heating affects both bulky and small compounds to the same extent. Therefore, in our opinion Joule heating did not cause the abnormal broadening peaks of bulky molecules.

As a result, it is obvious that for bulky molecules mass transfer is the predominant factor to plate height. Under high temperature, the mass transfer can be greatly speeded up by the increase in their diffusion coefficients, and consequently the column efficiency can be enhanced substantially.

3.3. Comparison between HPLC and CEC

Columns were also investigated under pressure-driven mode. Fig. 11 shows the Van Deemter curves for thiourea under both CEC and μ-HPLC conditions on column *c*. The calculated Van Deemter parameters *A* and *C* are 6.0 μm and 5.7×10^{-4} min under pressure- and 5.6 μm and 1.7×10^{-4} min under electro-driven conditions, respectively. As expected, the plate height under electro-driven conditions is much lower than that in the pressure mode. Furthermore, the plate height differences between the two modes become larger with the increase in the flow-rate due to the flat flow profile under electro-driven mode.

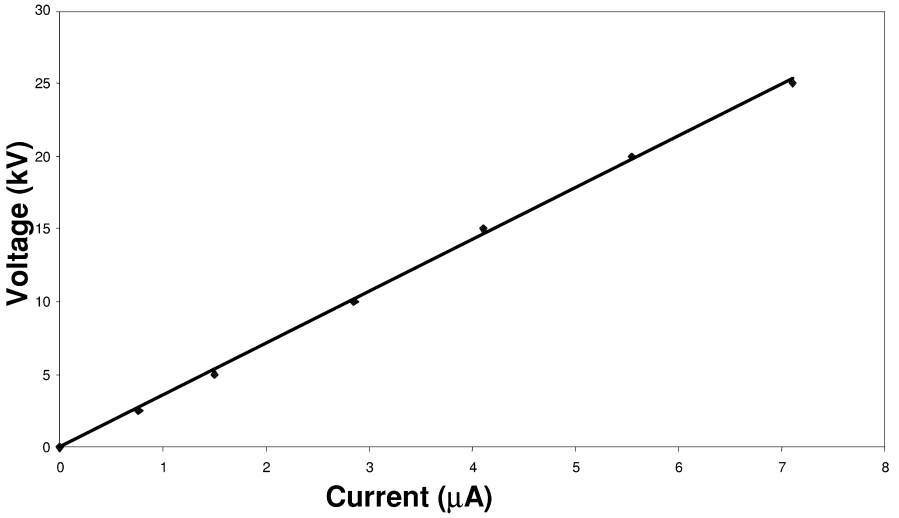

Fig. 10. Plot of voltage versus current for column *d*. Conditions are as in Fig. 1.

As an example, a comparison of chromatograms on column *c* for various test compounds under both modes is shown in Fig. 12. From the peak widths, the difference in column efficiency obtained under two eluent driven modes can be easily seen. The plate number under electro-driven conditions in Fig. 12A is more than twice that in the pressure-driven mode. Typical values for the plate numbers (plates per m) of peaks 2–12 are 40 000 under HPLC and 105 000 under CEC conditions. The retention factors of each compound in CEC (k_{CEC}) and μ-HPLC (k_{HPLC}) and their ratios (k_{HPLC}/k_{CEC}) are listed in Table 2. For the apolar and polar compounds in the test (Fig. 12A), the k_{HPLC}/k_{CEC} and the peak symmetry values (not shown) are close to one. These compounds show similar retention behaviors under both HPLC and CEC conditions. However, for compounds with higher polarity, e.g. benzylamine in Fig. 12B, the columns show completely different performance under the two eluent driven modes. Under CEC conditions, the benzylamine peak is extremely broad and tailing and it elutes later than under HPLC conditions. It is noteworthy to see that under the same conditions, the other basic compounds such as pyridine and *p*-ethylaniline show high-efficient and symmetric peaks (Fig. 12A). Clearly, this must be attributed to the pK_a-values of these compounds. The pK_a values of *p*-ethylaniline and pyridine are approximately 5; the pK_a-value of benzylamine is significantly larger (9.3). In the mobile phase of 80% acetonitrile and 20% phosphate buffer of pH 7 benzylamine is partly positively charged, which has been verified by capillary zone electrophoresis (CZE) experiments. Due to its electrophoretic mobility superimposition on the liquid chromatographic elution, benzylamine was expected to leave the column earlier under CEC condition compared to HPLC mode. However, this was not

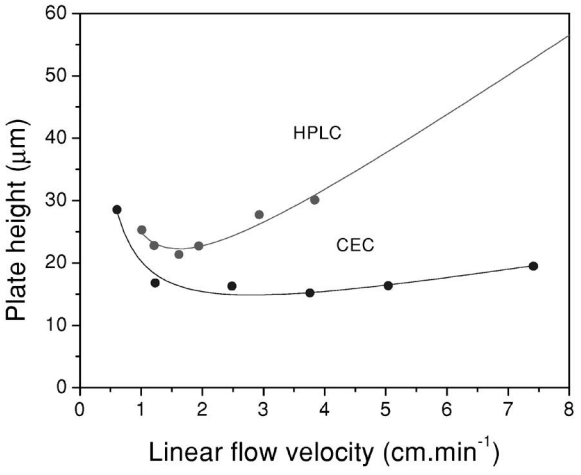

Fig. 11. Comparison of Van Deemter curves under electro- and pressure-driven conditions on column *c*. Column *c*: 41.5 cm (8.5 cm from detection window to outlet); sample, thiourea; temperature, 21°C; Other conditions are as in Fig. 1.

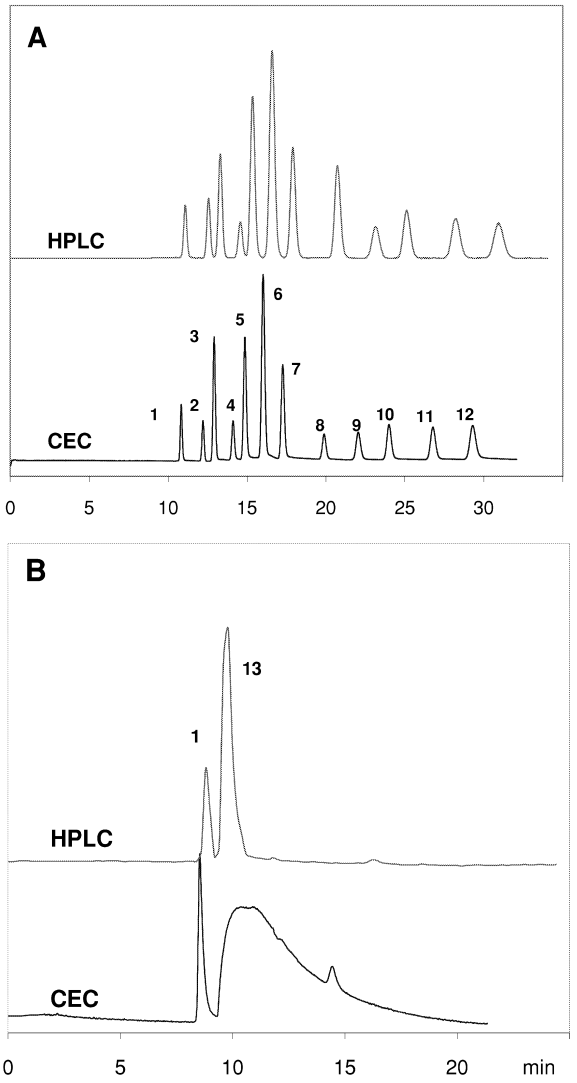

Fig. 12. Comparison of chromatograms on column *c* under electro- and pressure-driven conditions. Column *c*, 41.5 cm (8.5 cm from detection window to outlet). Sample: 1, thiourea; 2, pyridine; 3, benzylalcohol; 4, phenol; 5, aniline; 6, *p*-ethylaniline; 7, nitrobenzene; 8, benzene; 9, hexanophenone; 10, chlorobenzene; 11, propylbenzene; 12, biphenyl; 13, benzylamine. Separation conditions: temperature, 21°C; μ-HPLC, pressure drop: A, 150 bar; B, 185 bar. CEC, applied voltage: A, +11.5 kV; B, +15 kV.

observed in our experiments. We speculate that charged groups on the polymer were polarized and orientated in the electrical field. Under such a condition, the polymer may become more polar, and the interaction between benzylamine and polymeric stationary phase may be much stronger.

Table 3 shows the retention factor values of benzylamine on different columns under CEC and μ-HPLC. For columns *d* and *e* with higher phase ratios, the retention factor values are negative under CEC conditions; the higher the phase ratio, the smaller the retention factor. In contrast, on columns *b* and *c* with lower phase ratios, benzylamine has a positive retention factor and k_{CEC} is larger for the column with a smaller phase ratio. As discussed above, under the conditions used in this study benzylamine exists predominantly as a cation, so its retention is expected to be determined by both the electrophoretic migration and the interaction with the chromatographic stationary phase. On columns with a higher phase ratio, the retention of benzylamine is controlled by the electrophoretic effect but not by chromatographic influences; cations elute faster. In contrast, on columns with lower phase ratios, the retention of benzylamine is mainly attributed to reversed-phase chromatographic effects. Obviously, the strong interaction of benzylamine with polymer is responsible for the longer retention of benzylamine on columns *b* and *c* under CEC conditions.

3.4. Porosity

Total porosity (ϵ_T) is another important parameter for column evaluation. Various methods are available to measure ϵ_T, such as the flow method [55], applying chromatographic pressure-driven conditions, the conductivity method using electro-driven conditions [56], and the gravimetric method [57]. In this study, the flow method was used to measure ϵ_T-values. The calculation of ϵ_T was based on the equation $\epsilon_T = 4Ft_o/(d^2\pi L)$, where F is the volumetric flow-rate, t_o the retention time of an unretained marker (thiourea), d the column inner diameter, and L the column length. The average ϵ_T values at different flow-rates are given in Table 1. Considering the possible compressibility of some columns (see next section), a flow-rate lower than 0.5 μl/min was applied for ϵ_T-measurements. The relative standard deviation (RSD) of the measurement was less than 1.5%. Ideally, the porosity of a column is equal to the porogen volume fraction in the reaction solution. However, it is possible that some monomers may remain unreacted, some small polymer pieces may be soluble, and normally after polymerization the volume of highly cross-linked poly-

Table 2
Values of k_{HPLC}, k_{CEC} and k_{HPLC}/k_{CEC} of the test compounds in Fig. 11

	Compounds											
	2	3	4	5	6	7	8	9	10	11	12	13
k_{HPLC}	0.14	0.20	0.32	0.38	0.50	0.62	0.87	1.08	1.26	1.54	1.79	0.11
k_{CEC}	0.13	0.19	0.30	0.37	0.48	0.60	0.84	1.04	1.22	1.48	1.72	0.20
k_{HPLC}/k_{CEC}	1.05	1.04	1.04	1.03	1.04	1.04	1.04	1.04	1.03	1.04	1.04	0.55

Table 3
k_{HPLC} and k_{CEC} of benzylamine in CEC and micro-HPLC

	Column			
	b	*c*	*d*	*e*
Phase ratio	1.27	1.56	2.03	2.57
k_{HPLC}	0.14	0.11	0.08	0.05
k_{CEC}	0.30	0.20	−0.04	−0.20

mer is smaller than the volume of the starting monomers. As a result, the real ϵ_T is larger than the porogen volume fraction.

3.5. Reproducibility and stability

Reproducibility of various column parameters is a critical consideration in the field of preparation and application of rod columns. Therefore, a number of important parameters such as EOF, efficiency and retention factors were determined to test column-to-column as well as batch-to-batch reproducibility. The results of the reproducibility of EOF evaluated by the retention time of thiourea, the retention factor (k), and the column efficiency are summarized in Table 4. The day-to-day reproducibility of one column and the reproducibility of different columns were averaged from the results of 10 continuously repeating injections. Obviously, from Table 4, the reproducibility for both the EOF and the retention factor is satisfactory. In addition, the RSD values for column efficiency are acceptable, either for one batch or different batches. However, to apply these columns in daily routine practice further improvements to decrease variation in plate number should be made.

The mechanical stability of the columns was also studied. After using the columns for longer than 1 week, about 1-mm long empty parts at both ends of the column were observed. This was more obvious for columns prepared using high porogen content. Possible factors, such as EOF, pressure, and shrinkage that may affect the length of the polymer rod were systematically examined. It was found that the shrinkage of a polymer itself and the pressure might cause the polymer bed to become shorter. Under high pressure (up to 300 bar), columns with a porogen volume fraction of higher than 57% are compressible (Table 1). As can be concluded from the linear relationship between pressure drop and flow-rate, the polymer bed remains stable after column equilibration under high pressure. The column efficiency, however, decreases drastically after a column is compressed (Table 1). For columns *d* and *e*, the ratios of column efficiency after and before compression are 0.78 and 0.45, respectively. Hence,

Table 4
Reproducibility of electrochromatographic properties of column *c*

		RSD%			
		n	EOF	*k* (0.8–2.1)	Column efficiency
Single column	Run-to-run	10	0.26	<0.35	<1.52
	Day-to-day	6	0.78	<0.85	<3.54
Different columns	One batch	6	0.76	<3.90	<7.87
	Different batches	4	1.28	<1.84	<4.07

it is worthwhile noting that a low flow-rate should be applied for conditioning these CEC columns if a pump is used. However, when a modified fused-silica capillary is used pretreated with an acrylic double bond on the inner wall, both shrinkage and compressibility of the columns can be overcome. As seen in the SEM photo in Fig. 13, the polymer monolith in this column is covalently bounded to the inner wall of the capillary. There is no cleft between the polymer rod and the inner wall, which significantly differs from the SEM photos in Fig. 2. Therefore, modified capillaries may be a better alternative than unmodified fused-silica capillaries in preparation of monolithic columns.

3.6. Conclusion

Capillary monolithic CEC columns based on poly(alkylmethacrylate) with different phase ratios were prepared using different ratios of monomers to porogen. Small uniformly linked polymer microglobules were obtained for the columns at low porogen content. High efficiency up to 150 000 plates/m and high optimal flow velocity rates (up to ~6 cm/min) were achieved for all the test compounds with a wide range of retention factors. These columns are promising for fast analysis if a high voltage is used.

From the comparison of the column behavior under both electro- and pressure-driven modes, the higher efficiency and the flatter Van Deemter curve in CEC were observed as expected. The polymeric monolith in CEC demonstrated higher polarity possibly because the charged groups on polymer are polarized and become oriented under the electric field.

All the columns exhibit similar reversed-phase chromatographic retention mechanisms for most of the tested neutral compounds. For charged analytes under electro-driven conditions, a competition between chromatographic and electrophoretic retention was clearly seen. Moreover, for relatively bulky molecules columns show simultaneously size exclusion retention and chromatographic retention. In such a case, as long as the chromatographic partitioning is the leading force in the chromatographic process, the peaks are abnormally broad because of the slow mass transfer of bulky molecules, resulting from the steric resistance of micropores (<2 nm). This type of monolith is suitable for the analysis of very small molecules or macromolecules. In order to expand the application of these columns, it seems critical to enlarge the micropores to mesopore size similar to the inner pores of normal silica-based packing particles. Applications for the analysis of macromolecules and the preparation of new monoliths with mesopores are under development.

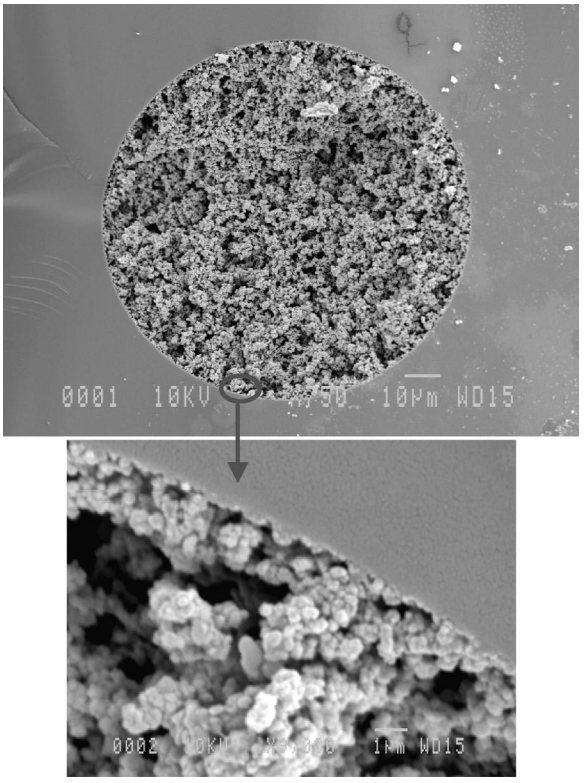

Fig. 13. SEM photos of a polymer rod column (*h*) with an inner wall modified fused-silica capillary.

Acknowledgements

The authors are grateful to N. Lousberg for SEM experiments and to A.P.B. Sommen for his assistance with micropore size measurements. We also acknowledge Dr X.W. Lou and Dr W.H. Ming for their beneficial discussions.

References

[1] J.H. Knox, I.H. Grant, Chromatographia 24 (1987) 135.
[2] J.H. Knox, I.H. Grant, Chromatographia 32 (1991) 317.
[3] M.M. Dittmann, G.P. Rozing, J. Chromatogr. A 744 (1996) 63.
[4] N.W. Smith, M.B. Evans, Chromatographia 38 (1994) 649.
[5] V. Pretorius, B.J. Hopkins, J.D. Schieke, J. Chromatogr. 99 (1974) 23.
[6] C. Yan, D. Schaufelberger, F. Erni, J. Chromatogr. A 670 (1994) 15.
[7] R. Stol, H. Poppe, W.Th. Kok, J. Chromatogr. A 887 (2000) 199.
[8] A.S. Rathore, Cs. Horváth, J. Chromatogr. A 781 (1997) 185.
[9] G. Choudhary, Cs. Horváth, J. Chromatogr. A 781 (1997) 161.
[10] A.S. Rathore, E. Wen, Cs. Horváth, Anal. Chem. 71 (1999) 2633.
[11] M.M. Dittmann, G.P. Rozing, J. Microcol. Sep. 9 (1997) 399.
[12] S.R. Witowski, R.T. Kennedy, J. Microcol. Sep. 11 (1999) 723.
[13] R. Stol, W.T. Kok, H. Poppe, J. Chromatogr. A 853 (1999) 45.
[14] Y. Zhang, W. Shi, L. Zhang, H. Zou, J. Chromatogr. A 802 (1998) 59.
[15] D. Li, V.T. Remcho, J. Microcol. Sep. 9 (1997) 389.
[16] U. Tallarek, E. Rapp, T. Scheenen, E. Bayer, H. van As, Anal. Chem. 72 (2000) 2292.
[17] R.A. Carney, M.M. Robson, K.D. Bartle, P. Myers, J. High Resolut. Chromatogr. 22 (1999) 29.
[18] M.G. Cikalo, K.D. Bartle, M.M. Robson, P. Myers, M.R. Euerby, Analyst 123 (1998) 87R.
[19] J.S. Kowalczyk, Chem. Anal. (Warsaw) 41 (1996) 157.
[20] R. Stevenson, K. Mistry, I.S. Krull, Int. Lab. 11 (1998) 11C.
[21] L.A. Colón, Y. Guo, A. Fermier, Anal. Chem. 8 (1997) 461A.
[22] T. Tsuda, Analusis 26 (1998) M48.
[23] L.A. Colón, K.J. Reynolds, R.A. Maldonado, A.M. Fermier, Electrophoresis 18 (1997) 2162.
[24] K.D. Altria, N.W. Smith, C.H. Turnbull, Chromatographia 46 (1997) 664.
[25] C. Fujimoto, Trends Anal. Chem. 18 (1999) 291.
[26] I.S. Krull, A. Sebag, R. Stevenson, J. Chromatogr. A 887 (2000) 137.
[27] U. Pyell, J. Chromatogr. A 892 (2000) 257.
[28] F. Steiner, B. Scherer, J. Chromatogr. A 887 (2000) 55.
[29] C.A. Rimmer, S.M. Piraino, J.G. Dorsey, J. Chromatogr. A 887 (2000) 115.
[30] M. Pursch, C. Sander, J. Chromatogr. A 887 (2000) 313.
[31] K. Schmeer, B. Behnke, E. Bayer, Anal. Chem. 67 (1995) 3656.
[32] B. Boughtflower, T. Underwood, Chromatographia 38 (1995) 329.
[33] M.M. Dittmann, G.P. Rozing, G. Ross, T. Adam, K.K. Unger, J. Capillary Electrophor. 4 (1997) 201.
[34] M.T. Dulay, R.P. Kulkarni, R.N. Zare, Anal. Chem. 70 (1998) 5103.
[35] G. Chirica, V.T. Remcho, Electrophoresis 20 (1999) 50.
[36] O.L. Tang, B.M. Xin, M.L. Lee, J. Chromatogr. A 837 (1999) 35.
[37] N. Ishizuka, H. Minakuchi, K. Nakanishi, N. Soga, H. Nagayama, K. Hosoya, N. Tanaka, Anal. Chem. 72 (2000) 1275.
[38] N. Minakuchi, K. Nakanishi, N. Soga, N. Ishizuka, N. Tanaka, Anal. Chem. 68 (1996) 3498.
[39] S.M. Fields, Anal. Chem. 68 (1996) 2709.
[40] N. Ishizuka, H. Minakuchi, K. Nakanishi, N. Soga, K. Hosoya, N. Tanaka, J. High Resolut. Chromatogr. 21 (1998) 477.
[41] F. Svec, E.C. Peters, D. Sýkora, C. Yu, J.M.J. Fréchet, J. High Resolut. Chromatogr. 23 (2000) 3.
[42] I. Gusev, X. Huang, Cs. Horváth, J. Chromatogr. 855 (1999) 273.
[43] A. Palm, M.V. Novotný, Anal. Chem. 69 (1997) 4499.
[44] L. Schweitz, L.I. Andersson, S. Nilsson, J. Chromatogr. A 817 (1998) 5.
[45] A. Maruška, C. Ericson, A. Vegvari, S. Hjertén, J. Chromatogr. A 837 (1999) 25.
[46] C. Ericson, S. Hjertén, Anal. Chem. 71 (1999) 1621.
[47] C. Ericson, J. Holm, T. Ericson, S. Hjertén, Anal. Chem. 72 (2000) 81.
[48] C. Ericson, J.-L. Liao, K. Nakazato, S. Hjertén, J. Chromatogr. A 767 (1997) 33.
[49] C. Fujimoto, J. Kino, H. Sawada, J. Chromatogr. A 716 (1995) 107.
[50] E.C. Peters, M. Petro, F. Svec, J.M.J. Fréchet, Anal. Chem. 70 (1998) 2288.
[51] E.C. Peters, M. Petro, F. Svec, J.M.J. Fréchet, Anal. Chem. 70 (1998) 2296.
[52] E.C. Peters, M. Petro, F. Svec, J.M.J. Fréchet, Anal. Chem. 69 (1997) 3646.
[53] X. Huang, Cs. Horváth, J. Chromatogr. A 788 (1997) 155.
[54] H.A. Claessens, Characterization of Stationary Phases for Reversed-Phase Liquid Chromatography: Column Testing, Classification and Chemical Stability, Ph.D. Thesis, Eindhoven University of Technology, The Netherlands, 1999, p. 151.
[55] Cs. Horváth, H.J. Lin, J. Chromatogr. 126 (1976) 401.
[56] J. Bear, in: Dynamics of Fluids in Porous Media, Dover Publications, New York, 1988, p. 113.
[57] K.K. Unger, in: Porous Silica, its Properties and Use as Support in Columns Liquid Chromatography, Elsevier, Amsterdam, 1979, p. 171.